ELSEVIER

*Polymer* Vol. 37 No. 8, pp. 1353–1361, 1996

0032-3861/96/$15.00 + 0.00

# An *FT* i.r. study of reaction kinetics and structure development in model flexible polyurethane foam systems

**Michael J. Elwell and Anthony J. Ryan***
*Manchester Materials Science Centre, UMIST, Grosvenor Street, Manchester M1 7HS, UK*

**and Henri J. M. Grünbauer and Henry C. Van Lieshout**
*Urethanes Research and Development, Dow Benelux N.V., Herbert H. Dow Weg, Postbus 48, 4530 AA Terneuzen, The Netherlands*
*(Received 21 March 1995; revised 24 July 1995)*

Forced-adiabatic, *FT* i.r. spectroscopy has been employed to simultaneously monitor polymerization and microphase separation on model flexible polyurethane foam systems. The following combinations of hydroxy functional components were investigated: (1) polyether-polyol and water; (2) polyether-polyol and deuterium oxide; (3) polyether-monol and water; and (4) polyether-monol and deuterium oxide. The formation of urethane, soluble urea, soluble D-urea, hydrogen-bonded urea and associated D-urea species were monitored during their fast bulk copolymerization with a diisocyanate. The decay of isocyanate is correlated to the polymerization kinetics and the evolution of hydrogen-bonded urea/associated D-urea is analysed emphasizing the onset of microphase separation of urea hard-segment sequences. The microphase separation transition (MST) occurred at a critical conversion of isocyanate functional groups. In the deuterium oxide blown foams, there was no trace of hydrogen-bonded urethane in the spectra obtained. In the polyether-monol systems, a lower conversion of isocyanate was observed at the MST and an overall lower reaction conversion was also observed. 

**(Keywords: flexible polyurethane foam; kinetics; polymerization)**

## INTRODUCTION

The reactive processing of water-blown flexible polyurethane foam from liquid monomers and oligomers involves a complex combination of both chemical and physical events. In less than 5 min, a liquid mixture of relatively low molecular weight components is transformed into the supramolecular architecture of solid foam. Information regarding both the reaction kinetics and development of morphology during processing are essential, such that an objective description of the events taking place and ultimately selective control of the process can be achieved. Flexible polyurethane foam is formed by the simultaneous reaction between a diisocyanate with polyether polyol and water. Combination of these two exothermic reactions leads to the formation of a segmented block copoly(urethane-urea), of the $-(H_mS)_n-$ type. This is blown into a foam by the cogeneration of carbon dioxide gas evolved from the water–isocyanate reaction. As the polymerization proceeds, the core of the rising foam bun becomes self-insulated by the surrounding polymer and this has the effect of bringing the process to occur under quasi-adiabatic conditions. Reaction kinetic studies during foam formation with both toluene diisocyanate (TDI) and methylene diphenyl diisocyanate (MDI) have been conducted previously and the results are in the literature[1–5].

Analyses[6–8] of the final morphology present in flexible polyurethane foams employing small angle X-ray scattering (SAXS), dynamic mechanical spectroscopy (d.m.s.) and differential scanning calorimetry (d.s.c.) have shown them to exhibit a microphase separated morphology similar to that of segmented urethane elastomers. The development of morphology during foaming is complex[3]. As the chemical reactions proceed, the chain lengths ($N$, degree of polymerization) of all the products increase and the interaction parameters ($\chi$) can also change. Such changes can give rise to the system crossing thermodynamic boundaries, which results in a transition from an initial homogeneous (disordered) state into a microphase separated (ordered) state[9,10].

The resultant morphology is determined by the kinetic competition between polymerization and microphase separation[7,9,10]. *In-situ* investigations regarding the reaction kinetics and development of polymer structure in both flexible and rigid polyurethane foam are sparse[3,5,11,12]. In this paper, results are presented from investigations in which *FT* i.r. spectroscopy has been employed, under forced-adiabatic conditions, to obtain information on the reaction kinetics and the development of structure during foam formation in model systems.

* To whom correspondence should be addressed

Model reactions have been employed previously to investigate the reaction kinetics in urethane systems[13–20]. As far as we are aware, there are only five studies[1,21–24] in the literature where model reaction systems have been employed to study the development of polymer morphology in urethane foams. Rossmy and co-workers[21–23] showed that urethane formation in the early part of the foaming reaction was not important with regard to foam stability in flexible systems, by synthesizing foams from both reactive and non-reactive polyethers. Such foams had sufficient internal modulus to withstand foam collapse and support their own mass. Hocker[24] reported that the carbonyl group present in soluble urea (1715 $cm^{-1}$) interacts sooner with urethane carbonyls (1730 $cm^{-1}$) than that of soluble D-urea (1697 $cm^{-1}$). The use of deuterium oxide instead of water results in a shifting of the soluble D-urea and associated D-urea absorbance peaks to lower wavenumbers. This facilitates further exposure to the urethane absorbance peak; which was partly obscured by the soluble urea peak in the systems where water was used. The use of deuterium oxide enables the presence of hydrogen-bonded urethane species to be probed as a result of the large reduction in the extent of peak overlap. More recently, Artavia and Macosko[1] have used deuterium oxide for investigating microphase separation of D-urea hard-segment sequence lengths under isothermal and forced-adiabatic conditions via *FT* i.r. spectroscopy during foam formation.

In order to understand more fully the reaction chemistry and subsequent structure development processes during foam formation; model foaming reactions employing a mono-functional polyether have been investigated. In foam formulations which commonly employ a nominally tri-functional polyether protocol, this component has been substituted for a mono-functional polyether (or monol) of the same chemical composition as the polyether polyol (i.e. effectively one arm of the polyether polyol). This eliminates the presence of urethane covalent crosslinks and enables the effect of their absence on the structure development processes to be investigated. In addition, water has been replaced by deuterium oxide as the blowing agent; thus enabling the presence of hydrogen-bonded urethane species to be probed.

To study the polymerization of flexible polyurethane foam via infra-red spectroscopy is difficult. The material undergoes an exotherm of 75–150°C depending upon the water concentration, the viscosity of the reaction medium increases from approximately 10 to $10^{3.5-4}$ Pa s and the density decreases from 1000 to 30 kg $m^{-3}$ in under 4 min. Translated into volume, this means that the final foam volume is some 33 times greater than the initial volume. The reaction is highly exothermic and the amount of material required to achieve self-insulation cannot be contained within the standard sampling environment of a conventional infra-red spectrophotometer. Furthermore, because the samples are opaque, this results in the need for attenuated total reflectance (a.t.r.) as the sampling method for *FT* i.r. spectroscopy[1,2,4]. It is imperative that the temperature of the reflective element be identical to that of the bulk foam throughout the reaction exotherm. If not, and the temperature of the reflective element is lower than that of the foam material in contact with it, the reflective element acts as a heat sink and, as a consequence, will decrease the foam reaction exotherm, delay the reaction chemistry and disrupt the resulting morphological development. Rapid heating of the reflective element is necessary in order to replicate the reaction exotherm of the foam[1,2,4].

## EXPERIMENTAL

### *Materials*

A total of four formulations have been employed throughout the work. The following combinations of components were investigated: (1) polyether-polyol, water and diisocyanate; (2) polyether-polyol, deuterium oxide and diisocyanate; (3) polyether-monol, water and diisocyanate; (4) polyether-monol, deuterium oxide and diisocyanate. All are based upon 100.0 g polyol by convention. An isocyanate index of 105 was maintained throughout the work. Formulation details are reported in *Table 1*. All foaming systems were tested in triplicate. All chemicals were used as supplied. The polyol (polyether-polyol Voranol™ CP6001, The Dow Chemical Co.) was a nominally tri-functional block copolymer polyol of propylene oxide and ethylene oxide, with an equivalent weight of 2040 g $mol^{-1}$ by end group analysis[5]. The monol was a poly(ethylene oxide) tipped poly(propylene oxide) mono-functional polyether with an equivalent weight of 1996 g $mol^{-1}$ by end group analysis[5]. The blowing agents were deionized water and deuterium oxide (Janssen Chemica). The catalyst employed was DABCO™ 33LV (Air Products), and the surfactant Tegostab™ B4113 (Th. Goldschmidt). The diisocyanate was diphenyl methane diisocyanate. It is a 50:50 blend of the 4,4′ and 2,4′ isomers of MDI (composition determined by $^1$H n.m.r.[5]).

### FT *i.r. spectroscopy*

Polyol, deionized water, catalyst and surfactant were weighed, transferred into a 500 ml polystyrene cup and then stirred at 2500 rev $min^{-1}$ for 60 s using a mechanical

**Table 1** Details of the formulations employed for the forced-adiabatic, time-resolved *FT* i.r. spectroscopy measurements during foaming reactions

| Foaming system | % by weight hard-segment | Mass of polyol or monol (g) | Mass of isocyanate (g) | Mass of catalyst (g) | Mass of water or deuterium oxide (g) | Mass of silicone surfactant (g) |
|---|---|---|---|---|---|---|
| PU–220 | 24.5 | 100 | 38.7 | 0.70 | 2.20 | 0.80 |
| PU–220–MONOL | 24.4 | 100 | 38.7 | 0.70 | 2.20 | 0.80 |
| PU–$D_2O$–220 | 22.6 | 100 | 35.2 | 0.70 | 2.20 | 0.80 |
| PU–$D_2O$–220–MONOL | 22.6 | 100 | 35.3 | 0.70 | 2.20 | 0.80 |

agitator equipped with a triple blade impeller. Once the premixing step was completed, preweighed MDI was added to the polyol-water froth and the mixture was stirred at 2500 rev $min^{-1}$ for 8 s. Temperature and infra-red spectroscopy data acquisition were initiated simultaneously with the mechanical agitator for the mixing of the polyol–water froth and isocyanate.

Zinc selenide crystals of a cylindrical geometry with dimensions of 3.2 mm diameter and a length of 38.1 mm were employed. The number of effective reflections of the crystal was 10. For this application, the reflection element gave rise to quite high absorptions. In some cases the absorptions were too high and a large surface area of the crystal had to be shielded from exposure to polyurethane foam with the aid of aluminium foil. The infrared spectra were collected on a Bomem–Michelson MB-120 Fourier transform infra-red spectrophotometer equipped with a nitrogen cooled, mercury cadmium telluride (MCT) detector. Spectracalc™ software (Galactic Industries) was employed for all of the computer assisted data acquisition and subsequent data analysis. Infra-red spectra were collected at 8 $cm^{-1}$ resolution, co-adding six scans per file. A DSP-100 FFT (Fast Fourier transform) processor installed in a 386 MS-DOS computer allowed real time Fourier transformation of the interferograms, leading to a direct absorbance-frequency–time display.

Infra-red data for the background file were obtained at 8 $cm^{-1}$ resolution, co-adding 256 scans prior to the execution of a kinetic run. Temperature as a function of time was recorded using type J thermocouples (0.25 mm diameter, Omega Engineering Inc.). The thermocouple was accurate to ±0.1°C. The thermocouple was connected with a Camile™ (The Dow Chemical Co.) data acquisition and control box, linked to an IBM 386 PC. Temperature was recorded as a function of time over a period of 1000–1400 s at a frequency of 1 Hz. The attenuated total reflectance-based Axiom DPR-111 deep immersion probe (Axiom Analytical Inc.) was used to house the crystal[4]. At each side of the reflecting element were positioned two cylindrically fitting aluminium moulds (length 25 mm); each fitted with a high density wattage cartridge heater (50 W, length 25 mm). In addition, one of the moulds also housed a type J thermocouple.

The lower base of the probe was fitted with a tubular aluminium mould (thickness 8 mm) equipped with five cartridge heaters (100 W, length 100 mm) and a type J thermocouple. The thermocouples and cartridge heaters for both the crystal and the probe moulds were connected with a Camile™ (The Dow Chemical Co.) data acquisition and control box as described above. The Camile™ system (i.e. control box, computer and software) uses the temperature of the reaction mixture as the control temperature for the heating devices which are mounted in the probe housing. The probe was connected to the MCT detector and the *FT* i.r. spectrophotometer via an optical transfer assembly consisting of light guides and coupling assemblies. A more detailed account of the instrumentation that was employed is described elsewhere[4,25].

*Analysis of the infra-red measurements*

The zinc selenide crystal that was employed in this study is optically denser than the polyurethane foam sample and transmits the infra-red beam during the kinetic run. The energy loss that is observed at a given frequency can be taken as a measure of the reduction in concentration of the absorbing substance. In this particular case it is the isocyanate concentration. Quantification of this is based on the Lambert–Beer law[26]:

$$A \propto \varepsilon . c \tag{1}$$

where $A$ is the measured integrated absorbance, $\varepsilon$ is the molar absorptivity of the sample ($cm^2\ mol^{-1}$) and $c$ is the concentration of the sample ($mol\ cm^{-3}$). As a result of the large density change which occurs during the polymerization (bulk density changes from approx. 1000 to 30 $kg\ m^{-3}$), a ratio between the absorbance of interest, e.g. NCO (2300–2200 $cm^{-1}$), and that of an internal reference that does not change in concentration during the reaction [normally 2960 $cm^{-1}$ (C–H stretch in the $CH_2$ of the polyether) or 1600 $cm^{-1}$ (>C=C< in plane vibration in aromatic ring)] must be taken to compensate for the large change in density.

However, due to the slow wetting of the crystal, the NCO and the two reference absorptions *do* show an initial increase in absorbance. For normalization of the decay in the isocyanate absorbance, the >C=C< (1600 $cm^{-1}$) absorbance was used as the reference. The areas under the absorbance peaks were determined using Spectralcalc™ software. Baseline corrections were fitted to all absorbance peak area data.

Denoting $A_{NCO}$ as the absorbance of the isocyanate and $A_{ref}$ as the absorbance of the reference species, it can be shown that[3,26]

$$\mathcal{A} = \frac{A_{NCO}}{A_{ref}} = \frac{\varepsilon_1 C_{NCO}}{\varepsilon_2 C_{ref}} = \frac{C_{NCO}}{\beta} \tag{2}$$

$\beta$ is defined as a constant.

$$\beta = \frac{\varepsilon_1}{\varepsilon_2 C_{ref}}$$

The extent of reaction can be calculated from the following expression:

$$p(\text{NCO-IR}) = 1 - \frac{\mathcal{A}(t)}{\mathcal{A}_0} \tag{3}$$

where $\mathcal{A}_0$ is obtained by computing the ratio of the isocyanate integrated absorbance and that of the internal standard for the initial reliable data points; followed by the use of linear least squares analysis to evaluate $\mathcal{A}$ at zero time. The isocyanate conversion can also be obtained from the normalized temperature rise profile utilizing the adiabatic reactor method[1,3,4].

$$p(\text{NCO-ATR}) = \frac{r(T_t - T_0)}{\Delta T_{ad.calc.}} \tag{4}$$

$r$ = stoichiometric imbalance = 100/isocyanate index (5)

$$\Delta T_{ad.calc.} = \frac{\Delta H_r [\text{NCO}]_0}{C_p . \rho} \tag{6}$$

$$\Delta T_{ad.calc.} = \frac{\Delta H}{C_p . m_T} \tag{7}$$

where $\Delta H$ = total calculated heat evolved (J), $C_p$ = specific heat capacity, literature[27] value 1.81 $J\ g^{-1}{}^{\circ}C^{-1}$, $m_T$ = total formulation mass (g).

*Urea formation (The blowing reaction):*

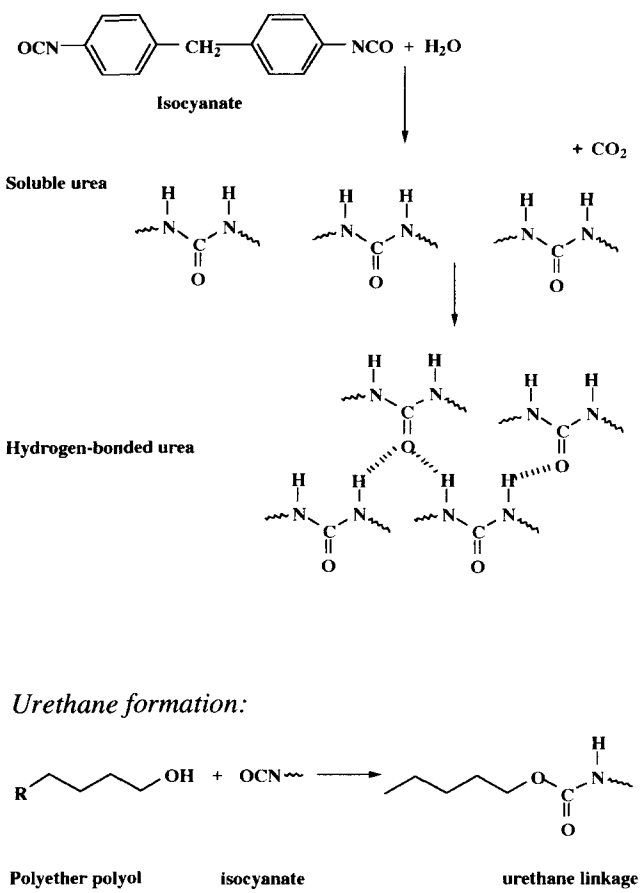


*Urethane formation:*




**Figure 1** Schematic representation of the reaction chemistry taking place during polyurethane foam formation

The literature[3] values for the enthalpy of reaction data used in this analysis are −93.9 and −146.6 kJ per mole of urethane and urea, respectively.

## RESULTS AND DISCUSSION

*Figure 1* shows the basic reaction chemistry that takes place during foam formation[4]. The isocyanate absorption band occurs at approximately 2300–2270 $cm^{-1}$ in the mid infra-red spectrum. The decay in the intensity of this absorbance can be used to monitor the conversion of isocyanate functional groups during the reaction. *Figure 2* shows a three-dimensional surface plot of absorbance vs frequency vs time for PU–220. Assuming that there are no side reactions[1,3,4], the only source of heat during the foaming reaction is that arising from consumption of the isocyanate functional groups. It is thus possible to correlate the isocyanate conversion calculated from the decay in the intensity of isocyanate absorbance with time, and that calculated from normalization of the reaction exotherm[1,3,4]. *Figure 3* shows a plot comparing isocyanate conversion calculated from the forced-adiabatic spectroscopy data (open symbols) with that calculated from the normalization of the foam reaction exotherm (solid line) for the foaming system PU–220. *Figure 4* shows the corresponding plot for the foaming system PU–$D_2O$–220–MONOL. It has been assumed

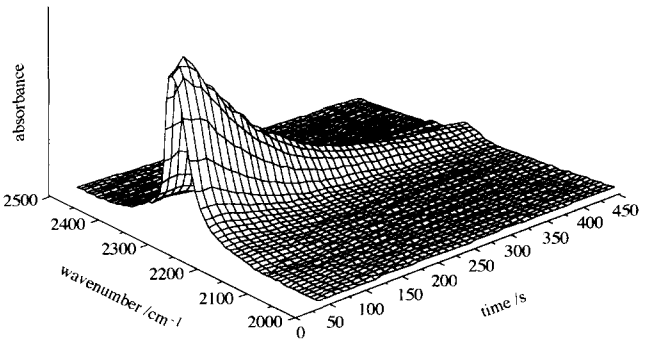


**Figure 2** Three-dimensional surface plot of absorbance vs frequency vs time for PU–220

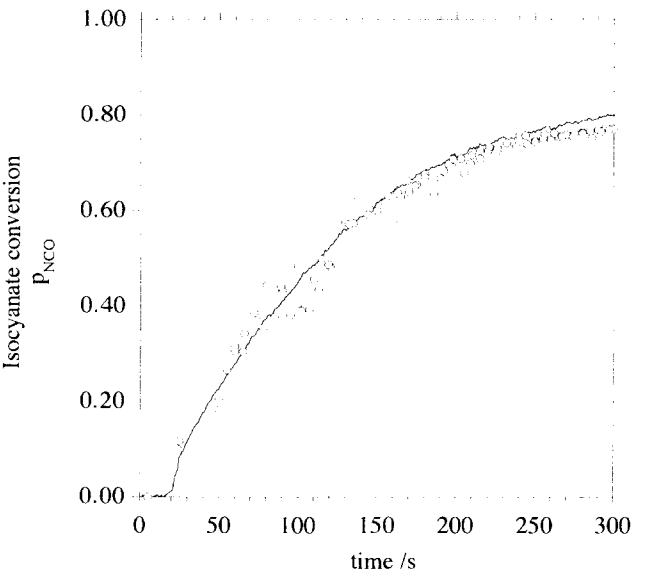


**Figure 3** Isocyanate conversion as a function of time showing the correlation between infra-red spectroscopy data (open symbols) and adiabatic temperature rise data (solid line) for PU–220

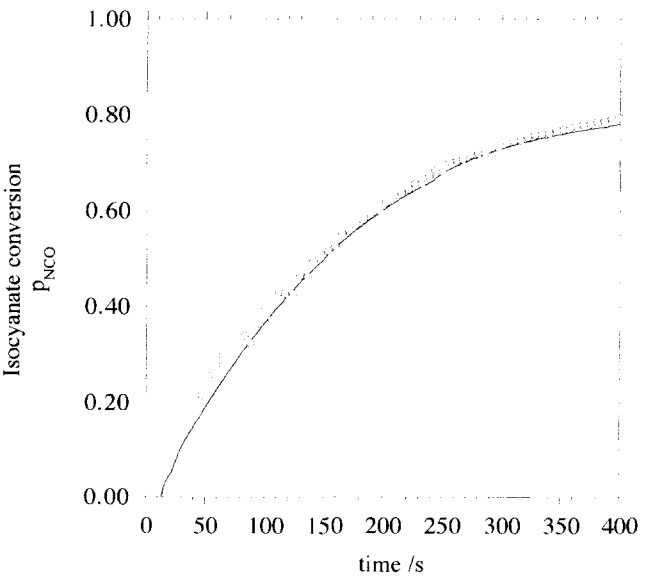


**Figure 4** Isocyanate conversion as a function of time showing the correlation between infra-red spectroscopy data (open symbols) and adiabatic temperature rise data (solid line) for PU–$D_2O$–220–MONOL

**Table 2** Infra-red band assignments observed in polyurethane foams

| Frequency ($cm^{-1}$) | Band assignment | Reference |
|---|---|---|
| 1730 | Free urethane | 28–32 |
| 1715–1710 | Soluble urea | 32 |
| 1697–1695 | Free urea | 24, 33 |
| 1661 | Intermediate urea | 30, 31 |
| 1645–1640 | H-bonded urea | 24, 29, 34 |
| 1710–1700 | H-bonded urethane | 2 |
| 1697 | Soluble D-urea | 1, 3, 24 |
| 1638 | Associated D-urea | 1, 3, 24 |

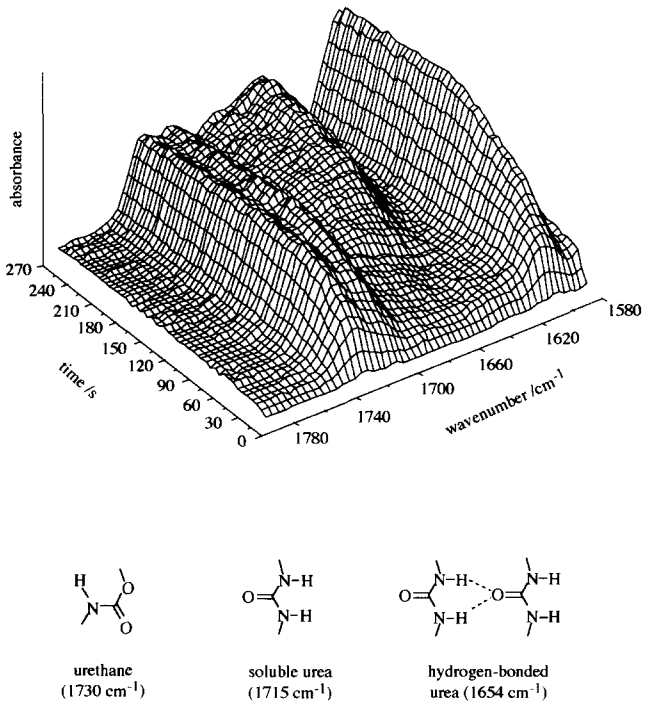


**Figure 5** Three-dimensional surface plot of absorbance vs frequency vs time for the region 1780–1580 $cm^{-1}$ in the mid infra-red spectrum for PU–220. The absorbances associated with urethane, soluble urea and hydrogen-bonded urea are indicated. The absorbance at ≈1600 $cm^{-1}$ is that associated with >C=C< in-plane vibration of the benzene ring

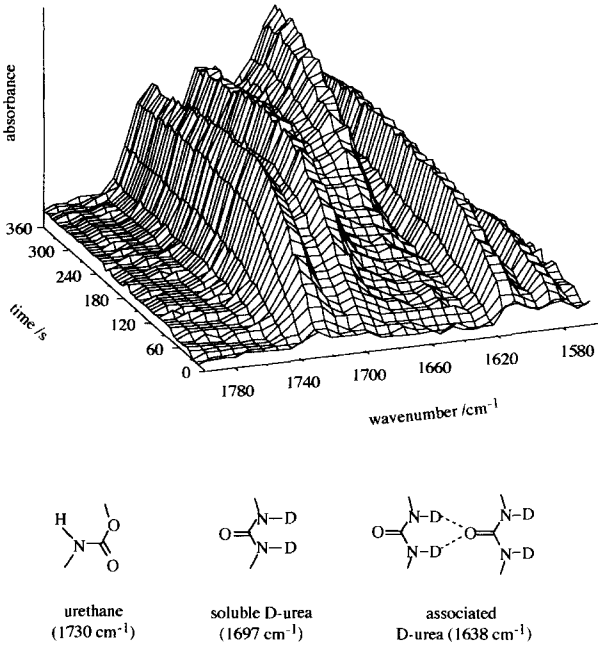


**Figure 6** Three-dimensional surface plot of absorbance vs frequency vs time for the region 1780–1580 $cm^{-1}$ in the mid infra-red spectrum for PU–$D_2O$–220. The absorbances associated with urethane, soluble D-urea and associated D-urea are indicated. The absorbance at ≈1600 $cm^{-1}$ is that associated with >C=C< in-plane vibration of the benzene ring

that the enthalpy of reaction for the formation of 1 mol of urea derived from deuterium oxide is equal to that for 1 mol of urea derived from water. As can be clearly observed from the two sets of curves, the correlation between the isocyanate conversion calculated from adiabatic temperature rise and infra-red spectroscopy data is within ±3% after approximately 40 s of the reaction. It should be noted that the first 15 s depicted on the aforementioned curves is associated with mixing of the components and loading of the reaction mixture into the infra-red cell arrangement.

The evolution of urethane, soluble urea and hydrogen-bonded urea during the foaming reaction can be followed by monitoring the carbonyl region of the mid infra-red spectrum. Several absorbances that occur in the carbonyl region have been assigned to specific functional groups, interactions and types of hydrogen bonding. *Table 2* presents the type of interaction, the frequency range at which the particular absorbance occurs and a reference to the assignment. *Figure 5* shows a three-dimensional surface plot of absorbance vs frequency vs time for the region 1780–1580 $cm^{-1}$ in the mid infra-red spectrum for the foaming system PU–220. The absorbances associated with urethane, soluble urea and hydrogen-bonded urea are indicated. The absorbance at approximately 1600 $cm^{-1}$ is that associated with >C=C< in-plane vibration of the benzene ring. It will be apparent that both urethane and soluble urea are evolved from an early point in the reaction. These two reactions take place simultaneously, not sequentially, as early research had suggested[22,28,35].

The use of deuterium oxide as the blowing agent, results in a shifting of the soluble D-urea and associated D-urea absorbance peaks to lower wavenumbers. This effect is clearly illustrated in *Figure 6*, which shows a three-dimensional surface plot of absorbance vs frequency vs time for the region 1780–1580 $cm^{-1}$ in the mid infra-red spectrum for the foaming system PU–$D_2O$–220. The absorbances associated with urethane, soluble D-urea and associated D-urea are indicated. The shifting of the soluble D-urea and associated D-urea absorbance peaks reduce the extent of peak overlap in the carbonyl region, and in turn, enable the presence of hydrogen-bonded urethane species (1710–1700 $cm^{-1}$)[2] to be probed. In both PU–$D_2O$–220 and PU–$D_2O$–220–MONOL there appeared to be no trace of hydrogen-bonded urethane. It was concluded that, if it is present, it is present in too low a concentration to be detected.

As in previous studies[1,3], the soluble urea absorbance and the hydrogen-bonded urea absorbance are employed to probe the strength of urea hydrogen bonding and, hence, the extent of microphase separation during the foaming reaction. Microphase separation occurs much earlier as the water concentration is increased[4,12] and this results from the increased rate of reaction arising from the increase in reactive functional group concentration. The ratio of urea groups to urethane groups has been

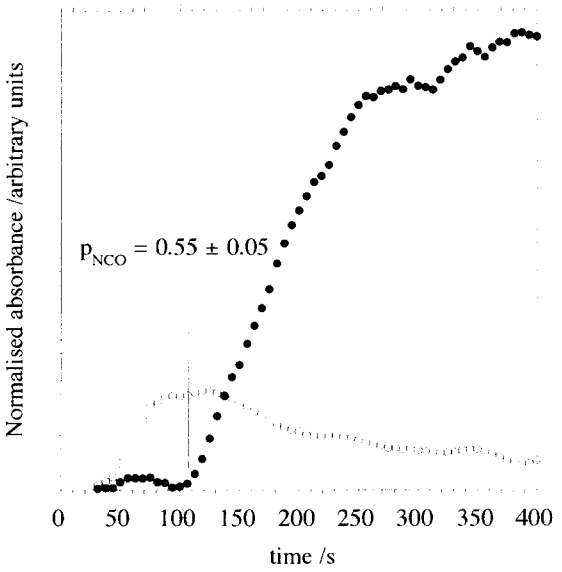


**Figure 7** Normalized soluble urea (open symbols) and normalized hydrogen-bonded urea (solid symbols) as a function of time for PU–220. The location of the MST is marked with a vertical arrow

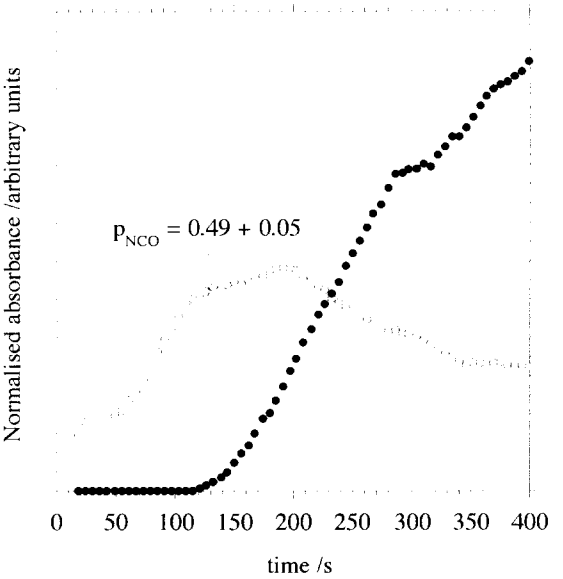


**Figure 8** Normalized soluble D-urea (open symbols) and associated D-urea (solid symbols) as a function of time for PU–$D_2O$–220. The location of the MST is marked with a vertical arrow

**Table 3** Conversion of isocyanate functional groups as the reaction time approaches 1000 s, overall relative initial rate of reaction between $p_{NCO}$ = 0.20 and 0.40, and conversion of isocyanate functional groups at which the MST occurs; for the different model foaming systems

| Foaming system | $p_{NCO}$ at $t \rightarrow 1000$ s | Overall relative initial rate of reaction ($s^{-1}$) | $p_{NCO}$ at the MST |
|---|---|---|---|
| PU–220 | 0.91 | 0.051 ± 0.002 | 0.55 ± 0.05 |
| PU–$D_2O$–220 | 0.86 | 0.038 ± 0.002 | 0.49 ± 0.05 |
| PU–220–MONOL | 0.82 | 0.047 ± 0.002 | 0.49 ± 0.05 |
| PU–$D_2O$–220–MONOL | 0.82 | 0.035 ± 0.003 | 0.39 ± 0.05 |

increased and the polyether soft-segment can only incorporate urea hard-segment sequences of a limited length before thermodynamic incompatibility results in microphase separation of the urea hard-segment sequence lengths. These subsequently undergo association resulting in strong hydrogen bonding interactions between the neighbouring urea groups.

*Figure 7* illustrates how normalized soluble urea (open symbols) and hydrogen-bonded urea (closed symbols) are evolved with time at 2.20 g water per 100.0 g polyol and *Figure 8* illustrates how normalized soluble D-urea (open symbols) and associated D-urea (closed symbols) are evolved with time at 2.20 g deuterium oxide per 100.0 g polyol. The soluble urea, soluble D-urea, hydrogen-bonded urea and associated D-urea absorbance bands were normalized against isocyanate conversion. The normalization is carried out because the probe (carbonyl) concentration is directly proportional to conversion. The normalization removes the change in concentration effect. The onset of microphase separation (MST) is indicated with an arrow and is taken as the point at which there is an acceleration in the hydrogen-bonded urea and a depletion in the free urea[1,29]. It has been observed[4,5] that across a broad range of water concentrations, the conversion of isocyanate functional groups at the MST remains approximately constant at $p_{NCO}$ = 0.55 ± 0.05. Thus, the critical isocyanate conversion at which the local number average hard-segment sequence length, $N_H$, reaches $N_{Hcrit}$, is approximately 55 ± 5% conversion of isocyanate functional groups, corresponding to an average hard-segment sequence length of 1.1–1.5[5].

From *Figure 8* it may be deduced that a similar type of structuring process occurs in PU–$D_2O$–220, as was observed in PU–220. The growth of the soluble D-urea concentration to critical threshold; at this point, microphase separation takes place followed by the subsequent growth of D-urea hard-segment sequences to evolve an interconnected physical network comprised of associated D-urea hard-segment sequences within a crosslinked polyether-urethane[4,12]. *Table 3* provides details of the mean value of the isocyanate conversion ($p_{NCO}$) at which the microphase separation transition was observed to occur in the different model foaming systems. The value quoted is the mean of three kinetic runs. From the data presented in *Table 3*, it is apparent that microphase separation occurs at a lower isocyanate conversion in PU–220–MONOL than in PU–220. However, the difference lies on the boundaries of the limits for experimental error. In the foaming systems PU–$D_2O$–220 and PU–$D_2O$–220–MONOL, it is quite clear that microphase separation occurs at a lower extent of isocyanate conversion in the case of the monol compared with that of the polyol.

During foaming with both water and deuterium oxide, the conversion of isocyanate functional groups at the

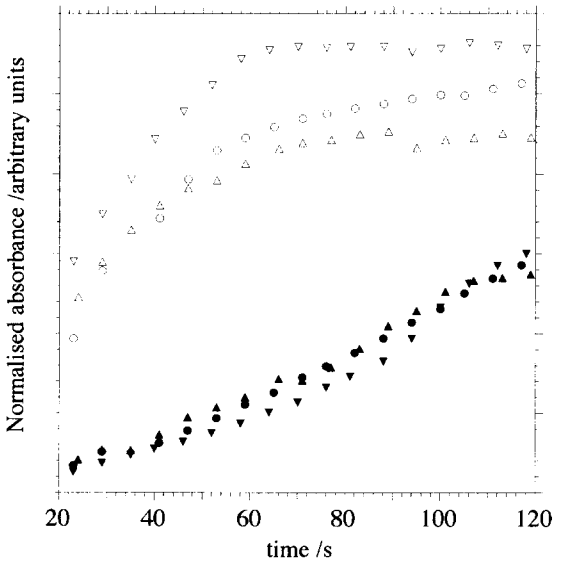


**Figure 9** Normalized absorbance as a function of time, illustrating the increase in concentration of urethane (open symbols) and soluble D-urea (solid symbols) for PU–$D_2O$–220–MONOL. The data shown are for three independent runs

MST is higher in the systems which contain polyol (PU–220 and PU–$D_2O$–220) compared with those which contain monol (PU–220–MONOL and PU–$D_2O$–220–MONOL). To identify the cause of this, firstly the relative overall initial rates of reaction were determined for each of the foaming systems. This was achieved by the fitting of a straight line to the conversion–time curve between $p_{NCO} = 0.20$ and 0.40. This region was selected so as to ensure that the analysis was applied to homogeneous reaction conditions, i.e. prior to the microphase separation transition (MST). The results that were obtained are given in *Table 3*. The relative rate of the $D_2O$–isocyanate reaction is slower than that of the water–isocyanate reaction for both polyol and monol foaming systems as a result of the lower concentration of deuterium oxide [0.110 mol] compared to water [0.122 mol].

In order to investigate the reaction sequences in terms of their relative rates of reaction in the model foaming systems, the areas under the absorbance peaks for the urethane, soluble urea and soluble D-urea were measured, normalized to the >C=C< absorbance and plotted as a function of time. *Figure 9* illustrates the evolution of urethane and soluble D-urea for three independent *FT* i.r. kinetic runs for the foaming system PU–$D_2O$–220–MONOL in the initial 120 s of reaction (i.e. before the MST). There is good agreement between the data on a run to run basis and it is apparent that in the initial stages of the reaction, both MDI tipped polyether oligomers and D-urea hard-segment sequences are present in the model foaming system PU–$D_2O$–220–MONOL. Similar behaviour was observed in all the model foaming systems and was reproducible on a run to run basis. Having analysed the chemistry of the model foaming systems both before the MST and beyond the MST, it is possible to attempt to explain the reason for the overall lower conversion of isocyanate functional groups observed in the mono-functional polyether based systems.

In PU–220, polymerization proceeds and from an early stage in the reaction there are isocyanate tipped polyether oligomers and urea hard-segment sequences present in the system (refer to *Figure 5*). The degree of polymerization of hard-segment, $N_H$, increases steadily and at $p_{NCO} = 0.55 \pm 0.05$, $N_H$ reaches $N_{Hcrit}$ and microphase separation takes place[4,12] (refer to *Figure 7*). Polymerization has provided the thermodynamic quench passing from the homogeneous (disordered) one-phase region to the heterogeneous (ordered) two-phase region. The microphase separated hard segments continue to grow and association of these urea hard segments occurs[4]. At $p_{NCO} = 0.71 \pm 0.02$, microphase separation is intercepted and quickly arrested by vitrification of the phase that is richer in hard-segment[4,36]. This phase has attained a composition with a $T_g$ equal to that of the surrounding polymer medium. It is the composition where liquid–liquid phase separation is intercepted and arrested by glass transition and is termed the Berghmans point[34]. In general foam terminology it is the physical gel point or end of rise time. Almost immediately after this, cell opening occurs. The vitrification of the hard segments 'freezes in' the morphology at that time and results in the evolution of a foam with an internal polymer morphology that comprises an interconnecting physical network of domains of hydrogen-bonded urea hard-segment sequences within the crosslinked polyether-urethane[12,36].

In PU–$D_2O$–220, from an early stage in the reaction there are isocyanate tipped polyether oligomers and soluble D-urea hard-segment sequences present in the system (refer to *Figure 6*). The degree of polymerization of D-urea hard-segment, $N_H$, increases steadily and at $p_{NCO} = 0.49 \pm 0.05$, $N_H$ reaches $N_{Hcrit}$ and microphase separation takes place (refer to *Figure 8*). The microphase separated D-urea hard segments continue to grow and association of these D-urea hard segments occurs[5]. At $p_{NCO} = 0.71 \pm 0.02$, microphase separation is intercepted and quickly arrested by vitrification of the phase that is richer in hard-segment[5].

In the mono-functional polyether systems the situation is somewhat different. In PU–22–MONOL, polymerization proceeds and as for the previous two systems, in the early stages of the reaction there are isocyanate-tipped polyether oligomers and urea hard-segment sequences present in the system[5,36]. The degree of polymerization of hard-segment, $N_H$, increases steadily and at $p_{NCO} = 0.49 \pm 0.05$, $N_H$ reaches $N_{Hcrit}$ and microphase separation takes place[38]. The microphase separated urea hard-segments continue to grow and association of these urea hard-segments occurs. However, in the monol system the rate of association of urea hard-segments is approximately 33% faster than in the polyol system[38]. This evidence is provided by values obtained for the effective diffusion coefficients from the *in-situ* synchrotron SAXS measurements[12,36,38]. Due to the very much faster rate of association of the urea hard-segments, aggregates of urea hard-segments will be formed which cannot be stabilized by the MDI tipped soft-segment oligomers acting as a surfactant. As a result, these aggregates undergo macrophase separation and become isolated entities that are not connected to the polyether matrix via a urethane linkage. At $p_{NCO} = 0.69 \pm 0.01$, phase separation is intercepted and quickly arrested by vitrification of the phase that is richer in hard-segment. The internal polymer morphology of the

polyether-monol foam systems are, for the greater part, similar to those of polyether-polyol foam systems[12,36,38]. Also dispersed within the interconnecting physical network of hydrogen-bonded urea hard-segment sequences and polyether-urethane are isolated larger aggregates of hydrogen-bonded urea hard-segment sequences.

Macrophase separation of the urea aggregates results in the entrapment of water/deuterium oxide molecules within the aggregates. The hard-segment sequences within these aggregates have pendant isocyanate functional groups which, once trapped within the isolated aggregate, encounter difficulty reacting with water/deuterium oxide or the remaining external population of polyether hydroxyl groups. It is highly probable that these groups are located at the two position and are of low reactivity[39,40]. This coupled with the increasing viscosity of the reaction medium beyond the Berghmans point[36,38] results in such species undergoing no further reaction. Further reaction between the remaining unreacted isocyanate groups that are *not* within macrophase separated urea aggregates will be controlled by translational and segmental diffusion and will require much molecular co-operation. The combined action of these effects results in a much reduced probability of reaction and hence, a much lower overall conversion of isocyanate functional groups in both PU–220–MONOL and PU–$D_2O$–220–MONOL is observed.

## SUMMARY AND CONCLUSIONS

It has been clearly demonstrated that in all the foaming systems investigated, from an early stage in the reaction there are isocyanate tipped polyether oligomers and urea hard-segment sequences present. The degree of polymerization of hard-segment, $N_H$, increases steadily, and when $N_H$ reaches $N_{Hcrit}$, microphase separation takes place. Polymerization has provided the thermodynamic quench passing from the homogeneous (disordered) one-phase region to the heterogeneous (ordered) two-phase region. For the polyether polyol–water systems, this appears to be at approximately $55 \pm 5\%$ conversion of isocyanate functional groups. The microphase separated urea hard segments continue to grow and association of these hard segments occurs. Since the onset of vitrification of the urea hard segments is observed to be at $p_{NCO} = 0.71 \pm 0.02$, the bulk of the microphase separation process occurs over the isocyanate conversion range of 50–73%. The replacement of water with deuterium oxide as the blowing agent resulted in a shifting of the soluble urea and associated urea absorbance peaks to lower wavenumbers, which in turn, enabled the presence of hydrogen-bonded urethane species to be probed. In both PU–$D_2O$–220 and PU–$D_2O$–220–MONOL, there appeared to be no trace of hydrogen-bonded urethane and it was concluded that if present, it is in too low a concentration to be detected.

In the monol systems, a lower conversion of isocyanate was observed at the MST and an overall lower conversion was also observed. The process of phase separation in the monol systems is somewhat different than in the polyol systems. It has been suggested that the lower degree of molecular connectivity between the microphases, coupled with the longer isocyanate conversion domain over which phase separation can take place in monols (22–30%), as compared to polyols (15–21%), results in a higher degree of microphase separation in the monols and also some degree of macrophase separation. In the foams synthesized with monols, the internal polymer morphology for the greater part is an interconnecting physical network of hydrogen-bonded urea hard segments within a polyether-urethane. In addition, within this are randomly dispersed larger aggregates of hydrogen-bonded urea hard-segment sequences.

The one major difference between the mono-functional and the nominally tri-functional based system is the molecular connectivity between the microphases in the polyol based systems (derived from the urethane covalent crosslinks) that is not present in the mono-functional based system. It is the absence of the covalent crosslinks that is responsible for there being no molecular connectivity between the microphases. Urethane covalent crosslinks are not a prerequisite for foam stability prior to the Berghmans point; however, beyond the Berghmans point the dimensional stability and the mechanical/physical properties of the foam are the prime requirements. To meet these criteria, *molecular connectivity between the microphases* via urethane covalent crosslinks is essential.

## ACKNOWLEDGEMENTS

MJE and AJR would like to thank Dow Benelux N.V., Terneuzen, The Netherlands for suggesting this problem and providing the necessary financial support. It is a pleasure to acknowledge Steven D. Henry for his help with the *FT* i.r. spectroscopy experiments.

## REFERENCES

1 Artavia, L. D. and Macosko, C. W. *J. Cell. Plast.* 1990, **26**, 490
2 Priester, R. D. Jr, McClusky, J. V., O'Neill, R. E., Turner, R. B., Harthcock, M. A. and Davis, B. L. *J. Cell. Plast.* 1990, **26**, 346
3 Artavia, L. D., Ph.D. Thesis, University of Minnesota, 1991
4 Elwell, M. J. A., Ryan, A. J., Grünbauer, H. J. M., Van Lieshout, H. C. and Thoen, J. A. *Prog. Rubb. Plast. Technol.* 1993, **9**, 120
5 Elwell, M. J. A., Ph.D. Thesis, Victoria University of Manchester, 1993
6 Turner, R. B., Spell, H. L. and Wilkes, G. L. 'Proc. 28th SPI Ann. Tech/Mrkt. Conf.', Technomic, Lancaster, PA, 1988, p. 244
7 Armistead, J. P., Turner, R. B. and Wilkes, G. L. *J. Appl. Polym. Sci.* 1988, **35**, 601
8 Creswick, M. W., Lee, K. D., Turner, R. B. and Huber, L. M. *J. Elast. Plast.* 1989, **21**, 179
9 Ryan, A. J. *Polymer* 1990, **31**, 707
10 Ryan, A. J., Stanford, J. L. and Still, R. H. *Plast. Rubb. Proc. Appl.* 1990, **13**, 99
11 Grünbauer, H. J. M., Thoen, J. A., Folmer, J. C. W. and Van Lieshout, H. C. *J. Cell. Plast.* 1992, **28**, 36
12 Elwell, M. J. A., Ryan, A. J. and Mortimer, S. *Macromolecules* 1994, **27**, 5428
13 Wong, S. W. and Frisch, K. C. *Prog. Rubb. Plast. Technol.* 1991, **7**, 243
14 Wong, S. W. and Frisch, K. C. *J. Polym. Sci., Part A: Polym. Chem.* 1986, **24**, 2867
15 Sorokin, M. F., Shode, L. G., Klochkova, L. V. and Finyakin, L. N. *Izv. Vyssh. Uchebn. Zaved., Khim. Khim. Tekhnol.* 1984, **27**, 852
16 Gus'kova N. A. and Sorokin, M. F. *Deposited Doc.* 1978, VINITI **12**, 321
17 Lipatova, T. E., Bakalo, L.A. and Chirkova, L.I. *Sint. Fiz.-Khim. Polim.* 1978, **23**, 74

18 Metlyakova, I. R. and Shoshtaeva, M. V. *Sint. Fiz.-Khim. Polim.* 1976, **18**, 48
19 Borkent, G. *Adv. Ureth. Sci. Technol.* 1974, **3**, 1
20 Grigor'eva, V. A., Baturin, S. M. and Entelis, S. G. *Vysokomol. Soedin., Ser. A.* 1972, **14**, 1345
21 Rossmy, G. R., Kollmeier, H. J., Lidy, W., Schator, H. and Wiemann, M. *J. Cell. Plast.* 1981, **17**, 319
22 Rossmy, G. R., Kollmeier, H. J., Lidy, W., Schator, H. and Wiemann, M. *J. Cell. Plast.* 1977, **13**, 26
23 Rossmy, G. R., Kollmeier, H. J., Lidy, W., Schator, H. and Wiemann, M. *J. Cell. Plast.* 1979, **15**, 276
24 Hocker, J. *J. Appl. Polym. Sci.* 1980, **25**, 2879
25 Axiom Analytical Incorporated, DPR-111 Deep Immersion Probe, Instruction Manual, Laguna Beach, March 1990
26 Griffith, P. R. and de Haseth, J. A. 'FT-IR Spectrometry', Wiley Interscience New York, 1986
27 Pannone, M. C. MSc. Dissertation, University of Minnesota, 1985
28 Bailey, F. E. and Critchfield, F. E. *J. Cell. Plast.* 1981, **17**, 333
29 Yang, W. P. and Macosko, C. W. *Makromol. Chem., Makromol. Symp.* 1989, **25**, 23
30 Christenson, C. P., Harthcock, M. A., Meadows, M. D., Spell, H. L., Harvard, W. L., Creswick, M. W., Guerra, R. and Turner, R. B. *J. Polym. Sci., Part B: Polymer. Phys. Edn* 1986, **24**, 1401
31 Hauptmann, G., Dörner, K. H. and Pfisterer, G. 'Proc. 5th SPI Annual Technical and Marketing Conf.', Technomic, Lancaster, PA, 1980, p. 617
32 Camargo, R. E., Macosko, C. W., Tirrell, M. and Wellinghoff, S. T. *Polym. Commun.* 1983, **24**, 314
33 Ishihara, H. I., Kimura, I., Saito, K. and Ono, H. *J. Macromol. Sci., Phys. Edn* 1984, **10**, 591
34 Burkhart, G., Kollmeier, H. J. and Schlöens, H. H. *J. Cell. Plast.* 1984, **20**, 37
35 Merten, R., Lauerer, D. and Dahm, M. *J. Cell. Plast.* 1968, **4**, 262
36 Elwell, M. J. A., Ryan, A. J., Grünbauer, H. J. M., Van Lieshout, H. C. and Lidy, W. *Plast. Rubb. Proc. Appl.* 1995, **23**, 265
37 Callister, S., Keller, A. and Hikmet, R. M. *Makromol. Chem. Makromol. Symp.* 1990, **39**, 19
38 Elwell, M. J. A., Ryan, A. J., Mortimer, S., Grünbauer, H. J. M. and Van Lieshout, H. C. *Macromolecules* in press
39 Brock, F. H. *J. Org. Chem.* 1959, **42**, 1802
40 Brock, F. H. *J. Phys. Chem.* 1961, **65**, 1638